



HAL
open science

Entropy-satisfying scheme for a hierarchy of dispersive reduced models of free surface flow

Martin Parisot

► **To cite this version:**

Martin Parisot. Entropy-satisfying scheme for a hierarchy of dispersive reduced models of free surface flow. 2018. hal-01242128v3

HAL Id: hal-01242128

<https://inria.hal.science/hal-01242128v3>

Preprint submitted on 26 Feb 2018 (v3), last revised 25 Jul 2019 (v4)

HAL is a multi-disciplinary open access archive for the deposit and dissemination of scientific research documents, whether they are published or not. The documents may come from teaching and research institutions in France or abroad, or from public or private research centers.

L'archive ouverte pluridisciplinaire **HAL**, est destinée au dépôt et à la diffusion de documents scientifiques de niveau recherche, publiés ou non, émanant des établissements d'enseignement et de recherche français ou étrangers, des laboratoires publics ou privés.

Entropy-satisfying scheme for a hierarchy of dispersive reduced models of free surface flow, Part I

Martin Parisot^{*1,2,3}

¹INRIA Paris, ANGE Project-Team, 75589 Paris Cedex 12, France

²Sorbonne Universités, UPMC Univ Paris 06, UMR 7598, Laboratoire Jacques-Louis Lions, F-75005, Paris, France

³CNRS, UMR 7598, Laboratoire Jacques-Louis Lions, F-75005, Paris, France

February 23, 2018

Abstract

This work is devoted to the numerical resolution in the multidimensional framework of a hierarchy of reduced models of the water wave equations. This article, the first in a series of two, focuses on a hierarchy of single-layer dispersive models, such as the Serre-Green-Naghdi model. A particular attention is paid to the dissipation of mechanical energy at the discrete level, i. e. the design of an entropy-satisfying scheme. To illustrate the accuracy and the robustness of the strategy, several numerical experiments are carried out. In particular, the strategy is capable of treating dry areas without special treatment.

1 Introduction

The propagation of surface waves is an essential issue for many applications such as port planning, tsunami propagation or marine energies. The dynamics of an incompressible, homogeneous and inviscid fluid is governed by the monovalued free surface Euler model (E), also known as water wave equations. Unfortunately, (E) is too complex to be simulated at the scale of applications and some processes such as the wet/dry front or the breaking wave can be numerically unstable. For geophysical applications, reduced models are widely used because they are easier and faster to solve numerically. The non-linear Shallow Water model (SW) is the simplest and most commonly used model nowadays. The main advantage of (SW) is its mathematical structure, i.e. hyperbolic, which has led to the design of effective

^{*}martin.parisot@inria.fr

numerical strategies, accurate (good description of shocks and wave speed [7, 19]) and robust (well balanced for several steady states [4, 10, 22, 27], entropy-satisfying [20, 30, 34], asymptotic preserving for several regimes [14, 28]). However, it is well known that (SW) is not a satisfactory model for wave propagation since dispersive effects are neglected. More precisely, the main assumptions for deriving (SW) from (E) are the so-called hydrostatic pressure in the fluid H_{yp}^p and the homogeneity of the horizontal velocity in the water column H_{yp}^u . These assumptions are described in more detail in §2.2.

In the past, some reduced models have been derived from (E) to circumvent these assumptions. The Serre-Green-Naghdi model (GN) , see [21, 29, 33], takes hydrodynamic pressure into account, i.e. bypasses H_{yp}^p . Several simplified models of it are proposed in the literature and in the following we also consider the non-hydrostatic model (NH) [8] since it is easily classifiable in a hierarchy explained in §2.2. All these models have the particularity of being dispersive and we call them dispersive models in the following.

To bypasses the second hypothesis H_{yp}^u , a layerwise discretization with mass exchange was proposed in [5]. This strategy seems particularly interesting because it preserves the mathematical structure of (SW) , at least for a small number of layers, see [1]. Recently, a layerwise version of the dispersive models has been proposed [17]. Note that the layerwise discretization is not the only strategy to bypass H_{yp}^u , see [9, 31, 32, 35].

All these models satisfy the conservation of the mechanical energy. This property is fundamental from the point of view of mathematics because it is an argument of stability for long time solution and for applications, particularly in renewable energies.

This work is devoted to the numerical resolution of the dispersive models. Several works in the literature deal with the resolution of these models. In [6, 12, 13], a numerical scheme is proposed based on a compact form of equations, i.e. where the only unknowns are the water depth and the horizontal velocity, using a splitting between the shallow water equations (SW) and the dispersive part of the equations. Despite the splitting strategy, third order derivatives still required to be discretized. Moreover, the compact form of the equation is not easily adaptable to the layerwise models. In [2, 3], the authors propose a developed form of (NH) , where the vertical-averaged vertical velocity is introduced. This new unknown added an equation to the hyperbolic step and limited the dispersive step to a second-order elliptical equation.

However, the dispersion step is solved by a pressure-based scheme and is not easily adaptable to (GN) . Indeed, for (GN) the hydrodynamic pressure has two degrees of freedom instead of one for (NH) , see 2.2.

In this paper, the first in a series of two, a new numerical strategy to solve the single-layer dispersive models is proposed. The novelty of the strategy lies in the proof of entropy stability. To our knowledge, this is the first numerical scheme for dispersive systems where the dissipation of numerical mechanical energy is proven.

In addition, the strategy provides a framework that is easily adaptable to *(NH)* or *(GN)*, and extensible to there layerwise versions. The numerical scheme for layerwise models are presented in a second paper, so we hope to present enough detail to clearly indicate the numerical method and present enough test cases to illustrate the behavior of the models.

This document is organized as follows. First, the free surface Euler model *(E)* is briefly presented in §2 as well as the hierarchy of reduced models. Then, §3 is devoted to the description of the numerical resolution within the multidimensional framework of each model in the hierarchy. The numerical scheme is built step by step with the complexity of the models. In §4, a simple treatment of the boundary conditions is presented. Eventually, several numerical illustrations in a one-dimensional frame are presented in §5 which validate the accuracy and robustness of the method.

2 The hierarchy of reduced models

2.1 Incompressible free surface Euler equations *(E)*

We consider an incompressible, homogeneous, inviscid free surface flow over a non-flat bathymetry subjected to the force of gravity. The frame (t, x, z) is such that $t \geq 0$ is the time, $x \in \Omega \subset \mathbb{R}^d$ is the coordinate of the horizontal plane with $d \in \{1, 2\}$, and $z \in \mathbb{R}$ is the vertical coordinate oriented in such a way that z increases upwards. The flow is supposed to satisfy the free surface incompressible Euler equations with a hypothesis of free surface monovalued. More precisely, the fluid is assumed to contain between a given lower surface $z = B(t, x)$ design as the bottom and an unknown free surface level $z = \eta(t, x) \geq B(t, x)$, and satisfies for any $B < z \leq \eta$

$$(E) \quad \begin{cases} \nabla \cdot u + \partial_z w = 0 \\ \partial_t u + (u \cdot \nabla) u + w \partial_z u = -\nabla p \\ \partial_t w + (u \cdot \nabla) w + w \partial_z w = -\partial_z p - g \end{cases}$$

with ∇ and $\nabla \cdot$ are respectively the gradient and the divergence according the x -variable, the horizontal velocity $u(t, x, z) \in \mathbb{R}^d$, the vertical velocity $w(t, x, z) \in \mathbb{R}$, the pressure in the fluid $p(t, x, z) \in \mathbb{R}$ and the gravity acceleration $g \in \mathbb{R}$. At bottom, the condition of non-penetration is taken into account, i.e.

$$\partial_t B + u|_{z=B} \cdot \nabla B = w|_{z=B}$$

and at free surface, the pressure is given by $p(t, x, \eta(t, x)) = P(t, x)$ and the kinematic condition is taken into account, i. e.

$$\partial_t \eta + u|_{z=\eta} \cdot \nabla \eta = w|_{z=\eta}.$$

The system of equation must be completed with an initial condition $\eta(0, x) = \eta^0(x)$, $u(0, x, z) = u^0(x, z)$ and $w(0, x, z) = w^0(x, z)$ which has to satisfied the compatibility

conditions with the divergence free condition and the boundary condition at bottom, i.e.

$$(1) \quad \nabla \cdot u^0 + \partial_z w^0 = 0 \quad \text{and} \quad \partial_t B|_{t=0} + u^0|_{z=B} \cdot \nabla B = w^0|_{z=B}.$$

For readability, we introduce the homogeneous potential

$$\phi(t, x) = gB(t, x) + P(t, x)$$

and the hydrodynamic pressure, also called non-hydrostatic pressure, defined by

$$q(t, x, z) = p(t, x, z) - P(t, x) - g(\eta(t, x) - z).$$

Let us recall the main physical properties of the Euler model (E).

Proposition 1. *Assuming $\eta^0(x) - B(0, x) \geq 0$, then the solution of (E) satisfies*

1.i) *the water depth positivity, i.e. $\eta(t, x) - B(t, x) \geq 0$.*

1.ii) *the mechanical energy conservation for a sufficiently smooth solution, i.e.*

$$\partial_t (\mathcal{E}(\eta - B) + \mathcal{K}^u + \mathcal{K}^w) + \nabla \cdot (\mathcal{G}^\eta + \mathcal{G}^u + \mathcal{G}^w + \mathcal{G}^q) = (\eta - B) \partial_t \phi + q|_{z=B} \partial_t B$$

with the potential energy

$$(2) \quad \mathcal{E}(h) = h \left(\phi + g \frac{h}{2} \right),$$

the kinetic energy $\mathcal{K}^\psi = \mathcal{K}(\eta, \psi)$ with

$$\mathcal{K}(\eta, \psi) = \int_B^\eta \frac{1}{2} |\psi|^2 dz,$$

and the flux are defined by $\mathcal{G}^\eta = \mathcal{G}(\eta, u, P + g\eta)$, $\mathcal{G}^u = \mathcal{G}(\eta, u, \frac{1}{2} \|u\|^2)$, $\mathcal{G}^w = \mathcal{G}(\eta, u, \frac{1}{2} |w|^2)$ and $\mathcal{G}^q = \mathcal{G}(\eta, u, q)$ with

$$\mathcal{G}(\eta, u, \psi) = \int_B^\eta \psi u dz.$$

2.2 Brief description of the single-layer models

In the current section, we present the hierarchy of single-layer reduced models of (E) that are considered in the sequel.

Shallow water model (SW)

First of all, we present (SW) [15] where the hydrodynamic pressure is neglected. The unknowns of (SW) are the water depth $h^{\text{SW}}(t, x) \in \mathbb{R}_+$ and the vertical-averaged

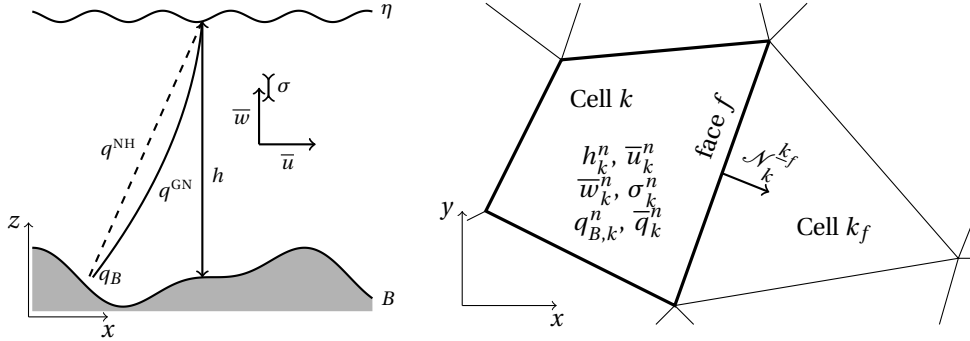


Figure 1: Illustration of the notations. (left) Interpretation of the unknowns in the vertical plan. (right) Finit volume discretization in the horizontal plan.

horizontal velocity $\bar{u}^{SW}(t, x) \in \mathbb{R}^d$, see Figure 1. More precisely, the unknowns of (E) are approximated by

$$\eta \approx B + h^{SW}, \quad u \approx \bar{u}^{SW}, \quad w \approx 0 \quad \text{and} \quad q \approx 0.$$

(SW) can be obtained from (E) mainly assuming that:

H_{yp}^p the pressure is hydrostatic, i.e. $p(t, x, z) \approx P(t, x) + g(\eta(t, x) - z)$.

H_{yp}^u the horizontal velocity is close to its vertical-average, i.e. $u(t, x, z) \approx \bar{u}(t, x)$.

A fine derivation from the Navier-Stokes equations is carried out in [18]. It is shown that (SW) is an approximation of a sufficiently smooth solution of Navier-Stokes equations in $O(\varepsilon)$ where ε is the ratio of the vertical characteristic length to the horizontal characteristic length. A higher order approximation can be derived, but it introduces dissipative terms.

Non-hydrostatic model (NH)

The simplest dispersive model subsequently considered (NH) [8]. In this approach, the vertical velocity is approached by its vertical-averaged and leads to a linear approximation of hydrodynamic pressure. The unknowns of (NH) are the water depth $h^{NH}(t, x) \in \mathbb{R}_+$, the vertical-averaged horizontal velocity $\bar{u}^{NH}(t, x) \in \mathbb{R}^d$, the vertical-averaged vertical velocity $\bar{w}^{NH}(t, x) \in \mathbb{R}$ and the hydrodynamic pressure at bottom $q_B^{NH}(t, x) \in \mathbb{R}$, see Figure 1. More precisely, the unknowns (u, w, q) of (E) are approximated in the vertical direction in $\mathbb{P}_0 \times \mathbb{P}_0 \times \mathbb{P}_1$ such that

$$\eta \approx B + h^{NH}, \quad u \approx \bar{u}^{NH}, \quad w \approx \bar{w}^{NH} \quad \text{and} \quad q \approx \frac{B + h - z}{h} q_B^{NH}.$$

A fine derivation of (NH) from (E) is realized in [8].

Serre-Green-Naghdi model (GN)

To satisfy the divergence free condition, the vertical velocity approximation must be of one order higher than the horizontal velocity. In the simple case, the horizontal velocity is approached in the vertical direction by means of a constant function, then the vertical velocity by means of a linear function and the hydrodynamic pressure by means of a quadratic function. It yields to (GN) [21, 29, 33]. The unknowns of (GN) are the water depth $h^{\text{GN}}(t, x) \in \mathbb{R}_+$, the vertical-averaged horizontal velocity $\bar{u}^{\text{GN}}(t, x) \in \mathbb{R}^d$, the vertical-averaged vertical velocity $\bar{w}^{\text{GN}}(t, x) \in \mathbb{R}$, the oriented standard deviation of the vertical velocity $\sigma^{\text{GN}}(t, x) \in \mathbb{R}$, the hydrodynamic pressure at bottom $q_B^{\text{GN}}(t, x) \in \mathbb{R}$ and the vertical-averaged hydrodynamic pressure $\bar{q}^{\text{GN}}(t, x) \in \mathbb{R}$, see Figure 1. More precisely, the unknowns (u, w, q) of (E) are approximated in the vertical direction in $\mathbb{P}_0 \times \mathbb{P}_1 \times \mathbb{P}_2$ such that

$$\eta \approx B + h^{\text{GN}}, \quad u \approx \bar{u}^{\text{GN}}, \quad w \approx \bar{w}^{\text{GN}} + 2\sqrt{3} \frac{z - B + \frac{h}{2}}{h} \sigma^{\text{GN}}$$

and $q \approx \frac{B + h - z}{h} q_B^{\text{GN}} + 3 \frac{(z - B)(B + h - z)}{h^2} (2\bar{q}^{\text{GN}} - q_B^{\text{GN}}).$

Other reconstructions of (E) unknowns from that of the Serre-Green-Naghdi model can be done in particular to satisfy a curl free condition of the divergence free condition. A finer derivation of (GN) from (E) and a more detailed description is performed in [23]. It is shown that (GN) is an approximation of (E) in the order of $O(\varepsilon^2)$ and $O(a)$ with a is the ratio between the characteristic wave amplitude and the characteristic water depth.

Other dispersive models, see [37], can be also considered and treated using a similar numerical strategy presented in the following. We limit the presentation to (NH) and (GN) for readability. For readability, the exponents SW, NH and GN are removed when the model used is not confusing. More precisely, each of the following subsections is devoted to a single model and the unknowns refer to it.

For each model, an entropy-satisfying scheme based on Finite volume discretization is proposed. Let us introduce some of the notations used in the following.

A tessellation \mathbb{T} of the horizontal domain $\Omega \subset \mathbb{R}^d$ is considered, composed of $N = \text{Card}(\mathbb{T})$ star-shaped control volumes, see Figure 1. One denotes by $k \in \mathbb{T}$ a cell, \mathbb{F}_k the set of its faces and $|k|$ its surface area. Furthermore, for a face f , its length is noted $|f|$ and the neighbor of k through f is denoted by \underline{k}_f such as $k \cup \underline{k}_f = f$. The unit normal to f outward to k is noted by $\mathcal{N}_k^{\underline{k}_f}$. To describe the schemes, the centered discrete operator $\nabla_k^\delta : (\mathbb{R})^N \rightarrow \mathbb{R}^d$ and $\nabla_k^\delta : (\mathbb{R}^d)^N \rightarrow \mathbb{R}$ are used respectively defined by

$$(3) \quad \nabla_k^\delta \psi = \frac{1}{|k|} \sum_{f \in \mathbb{F}_k} \frac{\psi_{\underline{k}_f} + \psi_k}{2} \mathcal{N}_k^{\underline{k}_f} |f|$$

and $\nabla_k^\delta \cdot \psi = \frac{1}{|k|} \sum_{f \in \mathbb{F}_k} \frac{\psi_k + \psi_{\underline{k}_f}}{2} \cdot \mathcal{N}_k^{\underline{k}_f} |f|.$

These discrete operators are clearly consistent with ∇ and $\nabla \cdot$ respectively and are second order. The time is discretized using an adaptive time step, i. e. $t^{n+1} = t^n + \delta_t^n$, with δ_t^n satisfying a CFL condition described below. The discrete unknowns ψ_k^n is the approximation of the mean value of the unknowns ψ in the cell k at time t^n . For readability, we introduce the discrete time derivative of a variable ψ by

$$(4) \quad \partial_t^{n+1} \psi = \frac{\psi^{n+1} - \psi^n}{\delta_t^n}.$$

3 Single-layer models

3.1 Shallow water model (SW)

3.1.1 Governing equations of (SW) and main properties

Let us begin the description of the strategy with the well-known shallow water model (SW). It reads

$$(SW) \quad \begin{aligned} \partial_t U^{SW} + \nabla \cdot F^{SW}(U^{SW}) &= S^{SW}(U^{SW}) \quad \text{with} \quad U^{SW} = \begin{pmatrix} h \\ h\bar{u} \end{pmatrix} \\ F^{SW}(U^{SW}) &= \begin{pmatrix} h\bar{u} \\ h\bar{u} \otimes \bar{u} + \frac{g}{2} h^2 \mathbf{I}_d \end{pmatrix} \quad \text{and} \quad S^{SW}(U^{SW}) = \begin{pmatrix} 0 \\ -h\nabla\phi \end{pmatrix}. \end{aligned}$$

The initial condition of (SW) is given by $h(0, x) = h^0(x)$ and $\bar{u}(0, x) = \bar{u}^0(x)$. Let us recall the main physical properties of (SW).

Proposition 2. *Assuming $h^0(x) \geq 0$, then the solution of (SW) satisfies*

2.i) *the water depth positivity, i.e. $h(t, x) \geq 0$.*

It is the counterpart of Proposition 1.i).

2.ii) *the mechanical energy conservation for a sufficiently smooth solution, i.e.*

$$\partial_t \left(\mathcal{E} + \overline{\mathcal{K}^u} \right) + \nabla \cdot \left(\overline{\mathcal{G}^h} + \overline{\mathcal{G}^u} \right) = h \partial_t \phi$$

with the potential energy $\mathcal{E}(h)$ defined by (2), the kinetic energy owing from the horizontal velocity $\overline{\mathcal{K}^u} = \overline{\mathcal{K}}(h, \bar{u})$ and the flux $\overline{\mathcal{G}^h} = \overline{\mathcal{G}}(h\bar{u}, \phi + gh)$ and $\overline{\mathcal{G}^u} = \overline{\mathcal{G}}(h\bar{u}, \overline{\mathcal{K}}(1, \bar{u}))$ with

$$(5) \quad \overline{\mathcal{K}}(h, \psi) = \frac{h}{2} \|\psi\|^2 \quad \text{and} \quad \overline{\mathcal{G}}(\mathcal{Q}, \psi) = \psi \mathcal{Q}$$

More precisely, in case of non-smooth solution, the admissible solution are defined such that the mechanical energy is decreasing, i.e.

$$\partial_t \left(\mathcal{E} + \overline{\mathcal{K}^u} \right) + \nabla \cdot \left(\overline{\mathcal{G}^h} + \overline{\mathcal{G}^u} \right) \leq h \partial_t \phi.$$

It is the counterpart of Proposition 1.ii).

3.1.2 Entropy-satisfying numerical scheme of (SW)

In the past, several numerical strategies have been proposed that preserve main physical properties, in particular Proposition 2. Dans le présent travail, nous rappelons brièvement l'un d'entre eux basé sur un schéma explicite de volume fini.

In the current work, we briefly recall one of them based on an explicit Finit Volume scheme. The scheme of (SW) can be formulate as

$$(SW^\delta) \quad U_k^{SW,n+1} = U_k^{SW,n} - \frac{\delta_t^n}{|k|} \sum_{f \in \mathbb{F}_k} \left(\mathcal{F}_f^{SW,n} \cdot \mathcal{N}_k^{k_f} + \mathcal{S}_{f,k}^{SW,n} \right) |f|$$

with $U_k^{SW,n} = (h_k^n, h_k^n \bar{u}_k^n)^t$. Several strategies are described in the literature to compute the numerical flux $\mathcal{F}_f^{SW,n} = \left(\mathcal{F}_f^{1,n} \cdot \mathcal{N}_k^{k_f}, \mathcal{F}_f^{2,n} \cdot \mathcal{N}_k^{k_f} \right)^t$ and the source term $\mathcal{S}_{f,k}^{SW,n}$ of the shallow water model, see [7, 19, 26, 36].

In the following, we ask (SW $^\delta$) to satisfy the following properties under a CFL condition like

$$(6) \quad \lambda \left(U_k^{SW,n}; U_{k_f}^{SW,n} \right) \delta_t^n \leq \min \left(\delta_k, \delta_{k_f} \right)$$

with δ_k the compactness of k_f , i.e. $\delta_k = \frac{|k|}{2}$ if $d = 1$ and $\delta_k = \frac{|k|}{\sum_{f \in \mathbb{F}_k} |f|}$ if $d = 2$. $\lambda(U_L^{SW}; U_R^{SW})$ is an upper limit of the wave speed, depending on the numerical flux \mathcal{F}^{SW} used, see [7].

Hypothesis 1. Under the CFL condition (6) and for any positive initial data, i.e. $h_k^0 \geq 0$, the solution of (SW $^\delta$) satisfies

1.i) the water depth positivity, i.e. $h_k^n \geq 0$.

It is the discrete counterpart of Proposition 2.i).

1.ii) the discrete mechanical energy dissipation. More precisely, there exist two flux $\bar{\mathcal{G}}_\delta^h(U_L^{SW}; U_R^{SW})$ and $\bar{\mathcal{G}}_\delta^{\bar{u}}(U_L^{SW}, U_R^{SW})$ respectively consistent with $\bar{\mathcal{G}}^h$ and $\bar{\mathcal{G}}^{\bar{u}}$ given in (5) such that the discrete mechanical energy satisfies

$$\partial_t^{n+1} \left(\mathcal{E}_k + \bar{\mathcal{K}}_k^{\bar{u}} \right) + \frac{1}{|k|} \sum_{f \in \mathbb{F}_k} \left(\bar{\mathcal{G}}_f^{h,n} + \bar{\mathcal{G}}_f^{\bar{u},n} \right) \cdot \mathcal{N}_k^{k_f} |f| \leq h_k^n \partial_t^{n+1} \phi_k$$

with $\mathcal{E}_k^n = \mathcal{E}(h_k^n)$, $\bar{\mathcal{K}}_k^{\bar{u},n} = \bar{\mathcal{K}}(h_k^n, \bar{u}_k^n)$, $\bar{\mathcal{G}}_f^{h,n} = \bar{\mathcal{G}}_\delta^h(U_k^{SW,n}, U_{k_f}^{SW,n})$ and $\bar{\mathcal{G}}_f^{\bar{u},n} = \bar{\mathcal{G}}_\delta^{\bar{u}}(U_k^{SW,n}, U_{k_f}^{SW,n})$.

It is the discrete counterpart of Proposition 2.ii).

For homogeneous potential, i.e. $\nabla \phi = 0$, some numerical strategies ensure the entropy stability Hypothesis 1.ii). This is the case, for example, of Godunov solver [20], of the kinetic solver [30] and of the Suliciu relaxation solver [34]. In the case of a source term, the numerical strategy only ensure a semi-discrete entropy stability,

i.e. before discretization in time, see [7]. Some implicit or ImEx schemes ensure the entropy stability with the source term, see instead [28], and can also be used with the numerical strategy of the dispersive models presented in the following.

Note that the Hypothesis 1 is not an exhaustive list of properties that we can ask for (SW), for instead the conservation of the steady state. Even if the translation of these properties at the discrete level is an interesting and stimulating question, this is not the purpose of the current work.

3.2 Non-hydrostatic model (NH)

3.2.1 Governing equations of (NH) and main properties

Let us now focus on the second assumption H_{yp}^p). The simplest model in the hierarchy presented in §refhierarchy is the non hydrostatic model (NH) which can be formulated as follows

$$(NH.a) \quad \begin{cases} \partial_t h + \nabla \cdot (h \bar{u}) & = 0 \\ \partial_t (h \bar{u}) + \nabla \cdot (h \bar{u} \otimes \bar{u} + \frac{g}{2} h^2 \mathbf{I}_d) + h \nabla \phi & = -\nabla \left(h \frac{q_B}{2} \right) - q_B \nabla B \\ \partial_t (h \bar{w}) + \nabla \cdot (h \bar{w} \bar{u}) & = q_B \end{cases}$$

with the hydrodynamic pressure q_B related to the constraint

$$(NH.b) \quad \bar{w} = \partial_t \left(B + \frac{h}{2} \right) + \bar{u} \cdot \nabla \left(B + \frac{h}{2} \right).$$

The initial condition $h(0, x) = h^0(x)$, $\bar{u}(0, x) = \bar{u}^0(x)$ and $\bar{w}(0, x) = \bar{w}^0(x)$ must satisfy the compatibility condition

$$(8) \quad \bar{w}^0 = \partial_t B|_{t=0} + \bar{u}^0 \cdot \nabla B - \frac{h^0}{2} \nabla \cdot \bar{u}^0$$

which corresponds to the vertical-averaged of the compatibility condition (1). For more detail about (NH), we refer to [8]. Let us first recall the main physical properties of (NH).

Proposition 3. *Assuming that $h^0(x) \geq 0$, then the solution of (NH) satisfies*

3.i) *the water depth positivity, i.e. $h(t, x) \geq 0$.
It is the counterpart of Proposition 1.i).*

3.ii) *the mechanical energy conservation for a sufficiently smooth solution, i.e.*

$$\partial_t \left(\mathcal{E} + \overline{\mathcal{K}^u} + \overline{\mathcal{K}^w} \right) + \nabla \cdot \left(\overline{\mathcal{G}^h} + \overline{\mathcal{G}^u} + \overline{\mathcal{G}^w} + \overline{\mathcal{G}^{q^{NH}}} \right) = h \partial_t \phi + q_B \partial_t B$$

*with the potential energy $\mathcal{E}(h)$ defined by (2), the kinetic energies $\overline{\mathcal{K}^\psi} = \overline{\mathcal{K}}(h, \psi)$, and the flux $\overline{\mathcal{G}^h} = \overline{\mathcal{G}}(h \bar{u}, \phi + gh)$, $\overline{\mathcal{G}^u} = \overline{\mathcal{G}}(h \bar{u}, \overline{\mathcal{K}}(1, \bar{u}))$, $\overline{\mathcal{G}^w} = \overline{\mathcal{G}}(h \bar{u}, \overline{\mathcal{K}}(1, \bar{w}))$, and $\overline{\mathcal{G}^{q^{NH}}} = \overline{\mathcal{G}}(h \bar{u}, \frac{q_B}{2})$ defined by (5).
It is the counterpart of Proposition 1.ii).*

3.2.2 Entropy-satisfying numerical scheme of (NH)

Now we focus on describing a numerical strategy for solving (NH) . As in previous works [2, 3, 6, 12, 24], the numerical scheme is based on a splitting strategy between the advection step and the dispersion step. The advantage of this strategy is to use the classic scheme (SW^δ) for the advection part. In particular, thanks to the formulation (NH) , the advection (left-hand side) of the vertical velocity is solved by conventional passive transport scheme. This strategy has already been used in [2, 3] and entropy-satisfying schemes to solve it can be used [7]. However, in the cited works, the dispersion step is solved using a prediction-correction strategy based on an implicit system on the hydrodynamic pressure q_B . Another strategy to solve the dispersive model is to write the equation on horizontal velocity, see [6, 12, 24]. The advantage of this strategy is that dissipative forces such as friction or viscous terms can also be taken into account simultaneously with dispersion. Unfortunately, without the introduction of vertical velocity, this strategy reveals third order derivatives that are not easy to discretize. The scheme proposed in the current work attempts to address the benefits of both strategies. More precisely, the vertical velocity is introduced and advected during the hyperbolic step and the dispersion step is resolved using an elliptical equation on the horizontal velocity. Other strategies based on a new set of variables was proposed in for example [16, 25] but it is not clear how to deal with source term such is bottom variation. Even if dissipative forces, friction and viscous terms, can be taken into account simultaneously with dispersion as in previous strategies based on horizontal velocity, we do not deal with these terms in this work for readability. We reformulated (NH) as

$$(9) \quad \begin{aligned} \partial_t U^{NH} + \nabla \cdot F^{NH}(U^{NH}) &= S^{NH}(U^{NH}) + D^{NH} \\ \text{with } U^{NH} &= \begin{pmatrix} U^{SW} \\ h\bar{w} \end{pmatrix}, \quad F^{NH}(U^{NH}) = \begin{pmatrix} F^{SW}(U^{SW}) \\ h\bar{w}\bar{u} \end{pmatrix} \\ S^{NH}(U^{NH}) &= \begin{pmatrix} S^{SW}(U^{SW}) \\ 0 \end{pmatrix} \quad \text{and} \quad D^{NH} = \begin{pmatrix} 0 \\ -\nabla(h\frac{q_B}{2}) - q_B\nabla B \\ q_B \end{pmatrix}. \end{aligned}$$

Let's now assume that the water depth, the horizontal velocity and vertical velocity at the time of iteration n are known, i.e. h_k^n , \bar{u}_k^n and \bar{w}_k^n , as for example at the initial condition. Then, the time step can be split into three steps, briefly described as follows:

1. The advection step $(NH^\delta.a)$, where the advection and the conservative forces are solved using (SW^δ) .
2. The dispersion step $(NH^\delta.b)$, where the dispersive operator, and eventually the dissipative forces, are solved using an implicit finite volume method.

Advection and conservative forces:

This step is based on (SW^δ) . More precisely, by neglecting the dispersal operator D^{NH} , the first two unknowns of U^{NH} are solution of (SW) while the third is simply

advected to the flow. This is a classic pollutant transport problem and a numerical strategy based on Suliciu relaxation [34] is commonly used. This strategy was already used for dispersive model in [2, 3]. We write

$$(NH^\delta.a) \quad U_k^{NH,n+1/2} = U_k^{NH,n} - \frac{\delta t}{|k|} \sum_{f \in \mathbb{F}_k} \left(\mathcal{F}_f^{NH,n} \cdot \mathcal{N}_k^{k_f} + \mathcal{S}_{f,k}^{NH,n} \right) |f|$$

with the state vector $U_k^{NH,n} = (U_k^{SW,n}, h_k^n \bar{w}_k^n)^t$, the source term $\mathcal{S}_{f,k}^{NH,n} = (\mathcal{S}_{f,k}^{SW,n}, 0)^t$, the numerical flux

$$\mathcal{F}_f^{NH,n} \cdot \mathcal{N}_k^{k_f} = \left(\begin{array}{c} \mathcal{F}_f^{SW,n} \cdot \mathcal{N}_k^{k_f} \\ \mathcal{F}_\delta^{up} \left(\mathcal{F}_f^{1,n} \cdot \mathcal{N}_k^{k_f}, (\bar{w}_k^n, \bar{w}_{k_f}^n) \right) \end{array} \right)$$

with the up-wind scheme

$$(11) \quad \mathcal{F}_\delta^{up}(Q, (\psi_L, \psi_R)) = \psi_L Q_+ - \psi_R Q_-$$

and the positive and negative part functions are defined by $\psi_\pm = \frac{|\psi| \pm \psi}{2}$.

Dispersion and dissipative forces:

Now let us introduce the scheme of the dispersion step. Since the water depth is not affected by this step, we have defined $h_k^{n+1} = h_k^{n+1/2}$. Then, wherever the water depth does not vanishes, the horizontal velocity is corrected by the following implicit linear scheme

$$(NH^\delta.b) \quad \alpha_k^{NH} \bar{u}_k^{n+1} + \nabla_k^\delta (\mu_k^{NH} \cdot \bar{u}^{n+1}) - \mu_k^{NH} \nabla_k^\delta \cdot \bar{u}^{n+1} - \nabla_k^\delta (\kappa_k^{NH} \nabla_k^\delta \cdot \bar{u}^{n+1}) = \beta_k^{NH}$$

with the discrete operators ∇_k^δ and $\nabla_k^\delta dot$ defined by (3) and the parameters

$$\begin{aligned} \alpha_k^{NH} &= h_k^{n+1/2} \left(\mathbf{I}_d + \nabla_k^\delta B^{n+1} \otimes \nabla_k^\delta B^{n+1} \right), \\ \mu_k^{NH} &= \frac{(h_k^{n+1/2})^2}{2} \nabla_k^\delta B^{n+1}, \quad \kappa_k^{NH} = \frac{(h_k^{n+1/2})^3}{4}, \\ \text{and } \beta_k^{NH} &= h_k^{n+1/2} \bar{u}_k^{n+1/2} + h_k^{n+1/2} \left(\bar{w}_k^{n+1/2} - \partial_t^{n+1} B_k \right) \nabla_k^\delta B^{n+1} \\ &\quad + \nabla_k^\delta \left(\frac{(h_k^{n+1/2})^2}{2} \left(\bar{w}_k^{n+1/2} - \partial_t^{n+1} B \right) \right). \end{aligned}$$

In the dry zone, the schema leads to a trivial equation and the resulting linear system is not well-posed. To overcome this issue, in all dry cells, $(NH^\delta.b)$ is replaced by $\bar{u}_k^{n+1} = 0$. The solution is obviously influenced by the choice of velocity in dry areas. However, this choice is motivated by the conservation of the mechanical energy at the dry front, see Proposition 4. More precisely, thanks to this choice, the energy flux

of the dispersive part vanishes on the dry front.

Finally, the vertical velocity is reconstructed using the following scheme

$$(NH^\delta.c) \quad \bar{w}_k^{n+1} = \partial_t^{n+1} B_k + \bar{u}_k^{n+1} \cdot \nabla_k^\delta B^{n+1} - \frac{h_k^{n+1}}{2} \nabla_k^\delta \cdot \bar{u}^{n+1}$$

where the discrete time derivative is defined by (4) and the discrete operators are defined by (3).

Let's explain how the scheme is obtained. $(NH^\delta.c)$ is obtained after a rewriting of $(NH.b)$ using the mass conservation (first equation of $(NH.a)$) as

$$\bar{w} = \partial_t B + \bar{u} \cdot \nabla B - \frac{h}{2} \nabla \cdot \bar{u}.$$

Even if other writings of the constraint can be considered, this one ensures the entropy stability, see Proposition 4. $(NH^\delta.b)$ is obtained by considering the following discretization of the dispersive operator

$$(13) \quad U_k^{NH,n+1} = U_k^{NH,n+1/2} + \delta_t^n \begin{pmatrix} 0 \\ -\nabla_k^\delta \left(h^{n+1} \bar{q}^{n+1} \right) - q_{B,k}^{n+1} \nabla_k^\delta B^{n+1} \\ q_{B,k}^{n+1} \end{pmatrix}.$$

Together with $(NH^\delta.c)$, they form a $(d+2) \times N$ linear system (without h). Fortunately, this system can be reduced by simple substitution and leads to the $d \times N$ linear system $(NH^\delta.b)$.

Proposition 4. *Assuming Hypothesis 1, $h_k^0 \geq 0$ and the CFL condition (6) holds. Then the solution of (NH^δ) satisfies*

4.i) *the water depth positivity, i.e. $h_k^n \geq 0$.*

It is the discrete counterpart of Proposition 3.i).

4.ii) *the discrete mechanical energy dissipation, i.e.*

$$\begin{aligned} & \partial_t^{n+1} \left(\mathcal{E}_k + \overline{\mathcal{K}}_k^{\bar{u}} + \overline{\mathcal{K}}_k^{\bar{w}} \right) \\ & + \frac{1}{|k|} \sum_{f \in \mathbb{F}_k} \left(\overline{\mathcal{G}}_f^{h,n} + \overline{\mathcal{G}}_f^{\bar{u},n} + \overline{\mathcal{G}}_f^{\bar{w},n} + \overline{\mathcal{G}}_f^{q^{NH,n+1}} \right) \cdot \mathcal{N}_k^{k_f} |f| \\ & \leq h_k^n \partial_t^{n+1} \phi_k + q_{B,k}^{n+1} \partial_t^{n+1} B_k \end{aligned}$$

with the energies $\mathcal{E}_k^n = \mathcal{E}(h_k^n)$, $\overline{\mathcal{K}}_k^{\psi,n} = \overline{\mathcal{K}}(h_k^n, \psi_k^n)$ defined by (5),

the flux $\overline{\mathcal{G}}_f^{h,n} = \overline{\mathcal{G}}_\delta^h \left(\begin{pmatrix} h_k^n \\ h_k^n \bar{u}_k^n \end{pmatrix}, \begin{pmatrix} h_{k_f}^n \\ h_{k_f}^n \bar{u}_{k_f}^n \end{pmatrix} \right)$, $\overline{\mathcal{G}}_f^{\bar{u},n} = \overline{\mathcal{G}}_\delta^{\bar{u}} \left(\begin{pmatrix} h_k^n \\ h_k^n \bar{u}_k^n \end{pmatrix}, \begin{pmatrix} h_{k_f}^n \\ h_{k_f}^n \bar{u}_{k_f}^n \end{pmatrix} \right)$ intro-

duced in Hypothesis 1.ii), $\overline{\mathcal{G}}_f^{\bar{w},n} = \mathcal{F}_\delta^{up} \left(\mathcal{F}_f^{1,n} \cdot \mathcal{N}_k^{k_f}, \left(\frac{(\bar{w}_k^n)^2}{2}, \frac{(\bar{w}_{k_f}^n)^2}{2} \right) \right)$ defined

by (11) and $\overline{\mathcal{G}}_f^{q^{\text{NH}},n} = \overline{\mathcal{G}}_\delta^q \left(\begin{pmatrix} h_k^n \\ \overline{u}_k^n \\ \frac{q_{B,k}^n}{2} \end{pmatrix}, \begin{pmatrix} h_{k_f}^n \\ \overline{u}_{k_f}^n \\ \frac{q_{B,k_f}^n}{2} \end{pmatrix} \right)$ defined by

$$\overline{\mathcal{G}}_\delta^q \left(\begin{pmatrix} h_L \\ u_L \\ \overline{q}_L \end{pmatrix}, \begin{pmatrix} h_R \\ u_R \\ \overline{q}_R \end{pmatrix} \right) = \frac{h_L \overline{q}_L + h_R \overline{q}_R}{2} \frac{\overline{u}_L + \overline{u}_R}{2} - \frac{h_R \overline{q}_R - h_L \overline{q}_L}{2} \frac{\overline{u}_R - \overline{u}_L}{2}.$$

It is the discrete counterpart of Proposition 3.ii).

Proof. Proposition 4.i) is an obvious consequence of Hypothesis 1.i).

Let's focus on mechanical energy conservation Proposition 4.ii). Thanks to Hypothesis 1.ii), we have

$$(14) \quad \mathcal{E}_k^{n+1/2} + \overline{\mathcal{K}}_k^{\overline{u},n+1/2} + \frac{\delta_t^n}{|k|} \sum_{f \in \mathbb{F}_k} \left(\overline{\mathcal{G}}_f^{h,n} + \overline{\mathcal{G}}_f^{\overline{u},n} \right) \cdot \mathcal{N}_k^{k_f} |f| \\ \leq \mathcal{E}_k^n + \overline{\mathcal{K}}_k^{\overline{u},n} + h_k^n (\phi_k^{n+1} - \phi_k^n)$$

with $\mathcal{E}_k^{n+1/2} = \mathcal{E}(h_k^{n+1/2})$ and $\overline{\mathcal{K}}_k^{\psi,n+1/2} = \overline{\mathcal{K}}(h_k^{n+1/2}, \psi_k^{n+1/2})$.

Similarly, a classical result of the Suliciu relaxation is the following entropy inequality as long as the positivity is ensured, see [7, Chapter 2.7]

$$(15) \quad \overline{\mathcal{K}}_k^{\overline{w},n+1/2} + \frac{\delta_t^n}{|k|} \sum_{f \in \mathbb{F}_k} \overline{\mathcal{G}}_f^{\overline{w},n} |f| \leq \overline{\mathcal{K}}_k^{\overline{w},n}.$$

Now, we focus on the dispersion step (NH^δ.b)-(NH^δ.c). As explained above, the dispersion step (NH^δ.b) is equivalent to (13). By multiplying the second equation of (13) by \overline{u}_k^{n+1} , it yields

$$(16) \quad \overline{\mathcal{K}}_k^{\overline{u},n+1} \leq \overline{\mathcal{K}}_k^{\overline{u},n+1/2} - \delta_t^n \left(\overline{u}_k^{n+1} \cdot \nabla_k^\delta \left(h^{n+1} \frac{q_B^{n+1}}{2} \right) + q_{B,k}^{n+1} \overline{u}_k^{n+1} \cdot \nabla_k^\delta B^{n+1} \right).$$

Thanks to the centered operator (3), the following relation holds

$$\overline{u}_k^{n+1} \cdot \nabla_k^\delta \left(h^{n+1} \frac{q_B^{n+1}}{2} \right) = \frac{1}{|k|} \sum_{f \in \mathbb{F}_k} \overline{\mathcal{G}}_f^{q^{\text{NH}},n+1} \cdot \mathcal{N}_k^{k_f} |f| - q_{B,k}^{n+1} \frac{h_k^{n+1}}{2} \nabla_k^\delta \cdot \overline{u}^{n+1}.$$

Then by multiplying the third equation of (13) by \overline{w}_k^{n+1} , it yields

$$(17) \quad \overline{\mathcal{K}}_k^{\overline{w},n+1} \leq \overline{\mathcal{K}}_k^{\overline{w},n+1/2} + \delta_t^n q_{B,k}^{n+1} \overline{w}_k^{n+1}.$$

Summing the energy dissipations (16) and (17), it yields

$$(18) \quad \overline{\mathcal{K}}_k^{\overline{u},n+1} + \overline{\mathcal{K}}_k^{\overline{w},n+1} + \frac{\delta_t^n}{|k|} \sum_{f \in \mathbb{F}_k} \overline{\mathcal{G}}_f^{q^{\text{NH}},n+1} \cdot \mathcal{N}_k^{k_f} |f| \leq \overline{\mathcal{K}}_k^{\overline{u},n+1/2} + \overline{\mathcal{K}}_k^{\overline{w},n+1/2} \\ + \delta_t^n q_{B,k}^{n+1} \left(\overline{w}_k^{n+1} - \overline{u}_k^{n+1} \cdot \nabla_k^\delta B^{n+1} + \frac{h_k^{n+1}}{2} \nabla_k^\delta \cdot \overline{u}^{n+1} \right).$$

Finally, we conclude by using $(NH^\delta.c)$. At wet/dry fronts, the water level vanishes in a cell, for instance $h_R = 0$. Then the energy flux is proportional to the velocity in the dry cell, i.e. $\overline{\mathcal{G}}_\delta^q = \frac{h_L \overline{q}_L}{2} \overline{u}_R$. By setting $\overline{u}_R = 0$, the flux through the wet/dry fronts vanishes. \square

Remark 1. *The dissipative term such are friction and viscosity can easily be treated simultaneously with dispersion. More precisely, it only adds the corresponding reaction and diffusion terms in $(NH^\delta.b)$.*

Remark 2. *A drawback of $(NH^\delta.b)$ is its large stencil, i. e. the 5-point stencil in 1D. Some may want to replace $(NH^\delta.b)$ with a more compact and simpler discrete operator, see Appendix A. However, the entropy stability Proposition 4.ii) is lost and in practice the numerical results are less accurate, see 5.3.*

Remark 3. *Some people may rather like to solve the linear system by keeping one of the other unknowns after substitution. For example, in [2, 3], the dispersion step is solved by maintaining the hydrodynamic pressure q_B as unknown to the linear system. This choice is particularly attractive for multidimensional simulations, since $\overline{u} \in \mathbb{R}^d$ whereas $q_B \in \mathbb{R}$. However, this formulation is less practical for imposing zero velocity in dry areas. Moreover, it is not possible to treat friction and viscosity, if any, in the same step, contrary to the formulation $(NH^\delta.b)$.*

3.3 Serre-Green-Naghdi model (GN)

3.3.1 Governing equations of (GN) and main properties

We are now dealing with the Serre-Green-Naghdi model [21, 29, 33]. To propose a scheme in the spirit of (NH^δ) , (GN) is reformulated as follows

$$(GN.a) \quad \begin{cases} \partial_t h + \nabla \cdot (h \overline{u}) & = 0 \\ \partial_t (h \overline{u}) + \nabla \cdot \left(h \overline{u} \otimes \overline{u} + \frac{g}{2} h^2 \mathbf{I}_d \right) & = -h \nabla \phi - \nabla (h \overline{q}) - q_B \nabla B \\ \partial_t (h \overline{w}) + \nabla \cdot (h \overline{w} \overline{u}) & = q_B \\ \partial_t (h \sigma) + \nabla \cdot (h \sigma \overline{u}) & = \sqrt{3} (2 \overline{q} - q_B) \end{cases}$$

with the hydrodynamic pressures \overline{q} and q_B related to constraints $(NH.b)$ and

$$(GN.b) \quad \sigma = \frac{\partial_t h + \overline{u} \cdot \nabla h}{2\sqrt{3}}.$$

The initial condition $h(0, x) = h^0(x)$, $\overline{u}(0, x) = \overline{u}^0(x)$, $\overline{w}(0, x) = \overline{w}^0(x)$ and $\sigma(0, x) = \sigma^0(x)$ must satisfy the compatibility conditions (8) and

$$(20) \quad \sigma^0 = -\frac{h^0}{2\sqrt{3}} \nabla \cdot \overline{u}^0$$

which corresponds to the vertical-averaged of the standard deviation of the compatibility condition (1). In [17] it is shown that (GN) is equivalent, at least for smooth solution, to the classical Peregrine formulation [29]. Let us first recall the main physical properties of (GN) .

Proposition 5. Assuming that $h^0(x) \geq 0$, then the solution of (GN) satisfies

5.i) the water depth positivity, i.e. $h(t, x) \geq 0$.
It is the counterpart of Proposition 1.i).

5.ii) the mechanical energy conservation for a sufficiently smooth solution, i.e.

$$\partial_t \left(\mathcal{E} + \overline{\mathcal{K}}^{\bar{u}} + \overline{\mathcal{K}}^{\bar{w}} + \overline{\mathcal{K}}^{\sigma} \right) + \nabla \cdot \left(\overline{\mathcal{G}}^h + \overline{\mathcal{G}}^{\bar{u}} + \overline{\mathcal{G}}^{\bar{w}} + \overline{\mathcal{G}}^{\sigma} + \overline{\mathcal{G}}^{q^{\text{GN}}} \right) = h \partial_t \phi + q_B \partial_t B$$

with the potential energy $\mathcal{E}(h)$ defined by (2), the kinetic energies $K^\psi = \overline{\mathcal{K}}(h, \psi)$ and the flux $\overline{\mathcal{G}}^h = \overline{\mathcal{G}}(h\bar{u}, \phi + gh)$, $\overline{\mathcal{G}}^{\bar{u}} = \overline{\mathcal{G}}(h\bar{u}, \overline{\mathcal{K}}(1, \bar{u}))$, $\overline{\mathcal{G}}^{\bar{w}} = \overline{\mathcal{G}}(h\bar{u}, \overline{\mathcal{K}}(1, \bar{w}))$, $\overline{\mathcal{G}}^{\sigma} = \overline{\mathcal{G}}(h\bar{u}, \overline{\mathcal{K}}(1, \sigma))$, $\overline{\mathcal{G}}^{q^{\text{GN}}} = \overline{\mathcal{G}}(h\bar{u}, \bar{q})$ defined by (5).
It is the counterpart of Proposition 1.ii).

3.3.2 Entropy-satisfying numerical scheme of (GN)

Now we focus on describing a numerical strategy for solving (GN). Similarly to (NH^δ), (GN.a) is written as

$$\begin{aligned} \partial_t U^{\text{GN}} + \nabla \cdot F^{\text{GN}}(U^{\text{GN}}) &= S^{\text{GN}}(U^{\text{GN}}) + D^{\text{GN}} \\ \text{with } U^{\text{GN}} &= \begin{pmatrix} U^{\text{NH}} \\ h\sigma \end{pmatrix}, \quad F^{\text{GN}}(U^{\text{GN}}) = \begin{pmatrix} F^{\text{NH}}(U^{\text{NH}}) \\ h\sigma u \end{pmatrix} \\ S^{\text{GN}}(U^{\text{GN}}) &= \begin{pmatrix} S^{\text{NH}}(U^{\text{NH}}) \\ 0 \end{pmatrix} \quad \text{and} \quad D^{\text{GN}} = \begin{pmatrix} 0 \\ -\nabla(h\bar{q}) - q_B \nabla B \\ q_B \\ \sqrt{3}(2\bar{q} - q_B) \end{pmatrix} \end{aligned}$$

and the numerical strategy is based on the same two steps: advection and conservative forces, dispersion and dissipative forces.

Advection and conservative forces:

As done for (NH^δ.a), the advection and conservative forces are realized using the strategy (SW^δ) with an up-wind scheme for the vertical velocities \bar{w}_k^n and σ_k^n . We write

$$(GN^\delta.a) \quad U_k^{\text{GN}, n+1/2} = U_k^{\text{GN}, n} - \frac{\delta_t^n}{|k|} \sum_{f \in \mathbb{F}_k} \left(\mathcal{F}_f^{\text{GN}, n} \cdot \mathcal{N}_k^{k_f} + \mathcal{S}_{f,k}^{\text{GN}, n} \right) |f|$$

with the state vectors $U_k^{\text{GN}, n} = (U_k^{\text{NH}, n}, h_k^n \sigma_k^n)^t$, the numerical flux

$$\mathcal{F}_f^{\text{GN}, n} \cdot \mathcal{N}_k^{k_f} = \begin{pmatrix} \mathcal{F}_f^{\text{NH}, n} \cdot \mathcal{N}_k^{k_f} \\ \mathcal{F}_\delta^{\text{up}} \left(\mathcal{F}_f^{1, n} \cdot \mathcal{N}_k^{k_f}, (\sigma_k^n, \sigma_{k_f}^n) \right) \end{pmatrix}$$

with the upwind flux defined by (11) and the source term $\mathcal{S}_{f,k}^{\text{GN}, n} = (\mathcal{S}_{f,k}^{\text{NH}, n}, 0)^t$.

Dispersion and dissipative forces:

As for (NH^δ) , we set $h_k^{n+1} = h_k^{n+1/2}$. In wet cell, i.e. $h_k^{n+1} > 0$, we write

$$(GN^\delta.b) \quad \alpha_k^{\text{GN}} \bar{u}_k^{n+1} + \nabla_k^\delta (\mu_k^{\text{GN}} \cdot \bar{u}^{n+1}) - \mu_k^{\text{GN}} \nabla_k^\delta \cdot \bar{u}^{n+1} - \nabla_k^\delta (\kappa_k^{\text{GN}} \nabla_k^\delta \cdot \bar{u}^{n+1}) = \beta_k^{\text{GN}}$$

where the parameters read

$$\alpha_k^{\text{GN}} = \alpha_k^{\text{NH}}, \quad \mu_k^{\text{GN}} = \mu_k^{\text{NH}}, \quad \kappa_k^{\text{GN}} = \frac{4}{3} \kappa_k^{\text{NH}} \quad \text{and} \quad \beta_k^{\text{GN}} = \beta_k^{\text{NH}} + \frac{1}{2\sqrt{3}} \nabla_k^\delta \left((h_k^{n+1/2})^2 \sigma_k^{n+1/2} \right).$$

and in dry cell we set $\bar{u}_k^{n+1} = 0$. Finally, the vertical velocity is reconstructed using $(NH^\delta.c)$ and

$$(GN^\delta.c) \quad \sigma_k^{n+1} = -\frac{h_k^{n+1}}{2\sqrt{3}} \nabla_k^\delta \cdot \bar{u}^{n+1}.$$

The scheme $(GN^\delta.b)$ was obtained similarly to $(NH^\delta.b)$. More precisely, the dispersive operator is discretized by

$$(22) \quad U_k^{\text{GN},n+1} = U_k^{\text{GN},n+1/2} + \delta_t^n \begin{pmatrix} 0 \\ -\nabla_k^\delta (h_k^{n+1} \bar{q}^{n+1}) - q_{B,k}^{n+1} \nabla_k^\delta B_k^{n+1} \\ q_{B,k}^{n+1} \\ \sqrt{3} (2\bar{q}_k^{n+1} - q_{B,k}^{n+1}) \end{pmatrix}$$

Together with $(GN^\delta.c)$, it forms a $(d+3) \times N$ linear system which can be reduced by simple substitution and leads to the $d \times N$ linear system $(GN^\delta.b)$.

Proposition 6. *Assuming Hypothesis 1, $h_k^0 \geq 0$ and the CFL condition (6) holds. Then the solution of (GN^δ) satisfies*

6.i) *the water depth positivity, i.e. $h_k^n \geq 0$.*

It is the discrete counterpart of Proposition 5.i).

6.ii) *the discrete mechanical energy dissipation, i.e.*

$$\begin{aligned} & \partial_t^{n+1} \left(\mathcal{E}_k + \overline{\mathcal{K}}_k^{\bar{u}} + \overline{\mathcal{K}}_k^{\bar{w}} + \overline{\mathcal{K}}_k^\sigma \right) \\ & + \frac{1}{|k|} \sum_{f \in \mathbb{F}_k} \left(\overline{\mathcal{G}}_f^{h,n} + \overline{\mathcal{G}}_f^{\bar{u},n} + \overline{\mathcal{G}}_f^{\bar{w},n} + \overline{\mathcal{G}}_f^{\sigma,n} + \overline{\mathcal{G}}_f^{q^{\text{GN},n+1}} \right) \cdot \mathcal{N}_k^{k_f} |f| \\ & \leq h_k^n \partial_t^{n+1} \phi_k + q_{B,k}^{n+1} \partial_t^{n+1} B_k \end{aligned}$$

with the energies $\mathcal{E}_k^n = \mathcal{E}(h_k^n)$, $\overline{\mathcal{K}}_k^{\psi,n} = \overline{\mathcal{K}}(h_k^n, \psi_k^n)$ defined by (5),

the flux $\overline{\mathcal{G}}_f^{h,n} = \overline{\mathcal{G}}_\delta^h \left(\begin{pmatrix} h_k^n \\ h_k^n \bar{u}_k^n \end{pmatrix}, \begin{pmatrix} h_{k_f}^n \\ h_{k_f}^n \bar{u}_{k_f}^n \end{pmatrix} \right)$, $\overline{\mathcal{G}}_f^{\bar{u},n} = \overline{\mathcal{G}}_\delta^{\bar{u}} \left(\begin{pmatrix} h_k^n \\ h_k^n \bar{u}_k^n \end{pmatrix}, \begin{pmatrix} h_{k_f}^n \\ h_{k_f}^n \bar{u}_{k_f}^n \end{pmatrix} \right)$ introduced in Hypothesis 1.ii), $\overline{\mathcal{G}}_f^{\bar{w},n} = \mathcal{F}_\delta^{\text{up}} \left(\mathcal{F}_f^{1,n} \cdot \mathcal{N}_k^{k_f}, \left(\frac{(\bar{w}_k^n)^2}{2}, \frac{(\bar{w}_{k_f}^n)^2}{2} \right) \right)$, $\overline{\mathcal{G}}_f^{\sigma,n} =$

$$\mathcal{F}_\delta^{up} \left(\mathcal{F}_f^{1,n} \cdot \mathcal{N}_k^{k_f}, \left(\frac{(\sigma_k^n)^2}{2}, \frac{(\sigma_{k_f}^n)^2}{2} \right) \right) \text{ defined by (11) and } \overline{\mathcal{G}}_f^{q^{GN},n} = \overline{\mathcal{G}}_\delta^{\overline{q}} \left(\begin{pmatrix} h_k^n \\ \overline{u}_k^n \\ \overline{q}_k^n \end{pmatrix}, \begin{pmatrix} h_{k_f}^n \\ \overline{u}_{k_f}^n \\ \overline{q}_{k_f}^n \end{pmatrix} \right)$$

is introduced in Proposition 4.ii).

It is the discrete counterpart of Proposition 5.ii).

Proof. Proposition 6.i) is an obvious consequence of Hypothesis 1.i).

Let us focus on the mechanical energy conservation Proposition 6.ii). The proof is similar to the one of Proposition 4.ii). Thanks to Hypothesis 1.ii), we obtain (14). Using the properties of the up-wind scheme, we obtain (15) and

$$(23) \quad \overline{\mathcal{K}}_k^{\sigma,n+1/2} + \frac{\delta_t^n}{|k|} \sum_{f \in \mathbb{F}_k} \overline{\mathcal{G}}_f^{\sigma,n} |f| \leq \overline{\mathcal{K}}_k^{\sigma,n}.$$

Now multiplying the second equation of (22) by \overline{u}_k^{n+1} , it reads

$$(24) \quad \begin{aligned} \overline{\mathcal{K}}_k^{\overline{u},n+1} + \frac{\delta_t^n}{|k|} \sum_{f \in \mathbb{F}_k} \overline{\mathcal{G}}_f^{q^{GN},n+1} \cdot \mathcal{N}_k^{k_f} |f| &\leq \overline{\mathcal{K}}_k^{\overline{u},n+1/2} \\ + \delta_t^n \left(\overline{q}_k^{n+1} h_k^{n+1} \nabla_k^\delta \cdot \overline{u}^{n+1} - q_{B,k}^{n+1} \overline{u}_k^{n+1} \cdot \nabla_k^\delta B^{n+1} \right). \end{aligned}$$

Then multiplying the third equation of (22) by \overline{w}_k^{n+1} , we get (17) and the fourth by σ_k^{n+1} , we get

$$(25) \quad \overline{\mathcal{K}}_k^{\sigma,n+1} \leq \overline{\mathcal{K}}_k^{\sigma,n+1/2} + \delta_t^n \sqrt{3} \left(2\overline{q}_k^{n+1} - q_{B,k}^{n+1} \right) \sigma_k^{n+1}$$

Summing the energy dissipations (24), (17) and (25), it yields

$$(26) \quad \begin{aligned} \overline{\mathcal{K}}_k^{\overline{u},n+1} + \overline{\mathcal{K}}_k^{\overline{w},n+1} + \overline{\mathcal{K}}_k^{\sigma,n+1} + \frac{1}{|k|} \sum_{f \in \mathbb{F}_k} \overline{\mathcal{G}}_f^{q^{GN},n+1} \cdot \mathcal{N}_k^{k_f} |f| \\ \leq \overline{\mathcal{K}}_k^{\overline{u},n+1/2} + \overline{\mathcal{K}}_k^{\overline{w},n+1/2} + \overline{\mathcal{K}}_k^{\sigma,n+1/2} + \delta_t^n 2\sqrt{3}\overline{q}_k^{n+1} \left(\sigma_k^{n+1} + \frac{h_k^{n+1}}{2\sqrt{3}} \nabla_k^\delta \cdot \overline{u}^{n+1} \right) \\ + \delta_t^n q_{B,k}^{n+1} \left(\overline{w}_k^{n+1} - \left(\overline{u}_k^{n+1} \cdot \nabla_k^\delta B^{n+1} + \sqrt{3}\sigma_k^{n+1} \right) \right). \end{aligned}$$

We conclude using (GN^δ.c) and summing with (14), (15) and (23). \square

Remark 4. Remarks 1 and 2 still holds for (GN^δ). Remark 3 still holds for (GN^δ) with a slight revision of the conclusion. The system could be solved either with $\overline{u} \in \mathbb{R}^d$ or with $(\overline{q}, q_B) \in \mathbb{R}^2$ as the main unknown. The first solution is clearly preferable while $d = 1$ in addition to the fact that the dry areas are treated simply.

4 Boundary conditions treatment

In this section, a simple treatment of boundary conditions is presented. Even at the continuous level, it is not clear what boundary conditions are compatible with

the dispersive models. We only present here the numerical processing of boundary conditions, i. e. how they are prescribed in practice. It is not clear that the following strategy is fully consistent with the ongoing framework and a rigorous analysis is required.

Let $\partial\mathbb{F}$ be the set of face at the boundary and for any $\tilde{f} \in \partial\mathbb{F}$ let $\tilde{k} \in \mathbb{T}$ be in the computational domain whereas its neighbor $\underline{\tilde{k}}_{\tilde{f}}$ is the ghost cell.

The advection step consists of the resolution of a system of hyperbolic equations. For a (not exhaustive) list of boundary conditions for (SW), see [19, Chapter V]. The dispersive models also required a boundary condition for \bar{w} and σ when the flow is incoming, i.e. $\mathcal{F}_{\tilde{f}}^{1,n} \cdot \mathcal{N}_{\tilde{k}}^{\tilde{k}_{\tilde{f}}} < 0$. In practice, we impose a value, usually zero, a the ghost cell.

Let us now focus on the dispersive step (GN^δ .b) (resp. NH^δ .b). Even if the horizontal velocity $\bar{u}_{\tilde{k}}^{n+1}$ is already known, several other unknown are required to write the scheme (GN^δ .b) (resp. NH^δ .b) in \tilde{k} . From (22) (resp. (13)), it is clear that only $\bar{q}_{\tilde{k}}^{n+1}$ (resp. $q_{B,\tilde{k}}^{n+1}$) is actually required. The strategy to impose the hydrodynamic pressure at the boundary was already propose in [2, 3]. In this paper, we only consider the Neumann condition $\bar{q}_{\tilde{k}}^{n+1} = \bar{q}_{\tilde{k}}^{n+1}$ (resp. $q_{B,\tilde{k}}^{n+1} = q_{B,\tilde{k}}^{n+1}$). More precisely, the scheme in the boundary cells \tilde{k} reads

$$\begin{aligned} & \alpha_{\tilde{k}}^{\text{xx}} \bar{u}_{\tilde{k}}^{n+1} + \frac{1}{2|\tilde{k}|} \left(\sum_{f \in \mathbb{F}_{\tilde{k}} \setminus \partial\mathbb{F}} \mu_{\tilde{k}_f}^{\text{xx}} \cdot \bar{u}_{\tilde{k}_f}^{n+1} \mathcal{N}_{\tilde{k}}^{\tilde{k}_f} |f| + \sum_{\tilde{f} \in \mathbb{F}_{\tilde{k}} \cap \partial\mathbb{F}} \mu_{\tilde{k}}^{\text{xx}} \cdot \bar{u}_{\tilde{k}}^{n+1} \mathcal{N}_{\tilde{k}}^{\tilde{k}_{\tilde{f}}} |\tilde{f}| \right) - \mu_{\tilde{k}}^{\text{xx}} \nabla_{\tilde{k}}^\delta \cdot \bar{u}^{n+1} \\ & - \frac{1}{2|\tilde{k}|} \left(\sum_{f \in \mathbb{F}_{\tilde{k}} \setminus \partial\mathbb{F}} \kappa_{\tilde{k}_f}^{\text{xx}} \nabla_{\tilde{k}_f}^\delta \cdot \bar{u}^{n+1} \mathcal{N}_{\tilde{k}}^{\tilde{k}_f} |f| + \sum_{\tilde{f} \in \mathbb{F}_{\tilde{k}} \cap \partial\mathbb{F}} \kappa_{\tilde{k}}^{\text{xx}} \nabla_{\tilde{k}}^\delta \cdot \bar{u}^{n+1} \mathcal{N}_{\tilde{k}}^{\tilde{k}_{\tilde{f}}} |\tilde{f}| \right) = \tilde{\beta}_{\tilde{k}}^{\text{xx}} \end{aligned}$$

with $\text{xx} = \text{NH}$ for (NH^δ), the parameters defined in (NH^δ .b) and

$$\begin{aligned} \mu_{\tilde{k}}^{\text{NH}} &= \frac{h_{\tilde{k}}^{n+1} h_{\tilde{k}}^{n+1}}{2} \nabla_{\tilde{k}}^\delta B^{n+1}, \quad \kappa_{\tilde{k}}^{\text{NH}} = \frac{h_{\tilde{k}}^{n+1} (h_{\tilde{k}}^{n+1})^2}{4}, \\ \tilde{\beta}_{\tilde{k}}^{\text{NH}} &= h_{\tilde{k}}^{n+1} \bar{u}_{\tilde{k}}^{n+1/2} + h_{\tilde{k}}^{n+1} \left(\bar{w}_{\tilde{k}}^{n+1/2} - \partial_t^{n+1} B_{\tilde{k}} \right) \nabla_{\tilde{k}}^\delta B^{n+1} \\ & + \frac{1}{4|\tilde{k}|} \left(\sum_{f \in \mathbb{F}_{\tilde{k}} \setminus \partial\mathbb{F}} \left(h_{\tilde{k}_f}^{n+1} \right)^2 \left(\bar{w}_{\tilde{k}_f}^{n+1/2} - \partial_t^{n+1} B_{\tilde{k}_f} \right) \mathcal{N}_{\tilde{k}}^{\tilde{k}_f} |f| \right. \\ & \left. + \sum_{\tilde{f} \in \mathbb{F}_{\tilde{k}} \cap \partial\mathbb{F}} h_{\tilde{k}}^{n+1} h_{\tilde{k}}^{n+1} \left(\bar{w}_{\tilde{k}}^{n+1/2} - \partial_t^{n+1} B_{\tilde{k}} \right) \mathcal{N}_{\tilde{k}}^{\tilde{k}_{\tilde{f}}} |\tilde{f}| \right). \end{aligned}$$

and $\text{xx} = \text{GN}$ for (GN^δ), the parameters defined in (GN^δ .b) and

$$\mu_{\tilde{k}}^{\text{GN}} = \mu_{\tilde{k}}^{\text{NH}}, \quad \kappa_{\tilde{k}}^{\text{GN}} = \frac{4}{3} \kappa_{\tilde{k}}^{\text{NH}},$$

$$\tilde{\beta}_k^{\text{GN}} = \tilde{\beta}_k^{\text{NH}} + \frac{1}{4\sqrt{3}|\tilde{k}|} \left(\sum_{f \in \mathbb{F}_{\tilde{k}} \setminus \partial\mathbb{F}} \left(h_{\tilde{k}_f}^{n+1} \right)^2 \sigma_{\tilde{k}_f}^{n+1/2} \mathcal{N}_{\tilde{k}}^{\tilde{k}_f} |f| + \sum_{\tilde{f} \in \mathbb{F}_{\tilde{k}} \cap \partial\mathbb{F}} h_{\tilde{k}_f}^{n+1} h_{\tilde{k}}^{n+1} \sigma_{\tilde{k}}^{n+1/2} \mathcal{N}_{\tilde{k}}^{\tilde{k}_f} |\tilde{f}| \right).$$

5 Numerical results

This section is devoted to numerical illustrations and comparisons between the models in one dimensional framework on a regular grid, i.e. for any $k \in \mathbb{T}$, $|k| = 2\delta_x$ with δ_x fixed and defined further. The gravitational acceleration is set to $g = 9.81$ for all following simulations. The advection step is computed using the widely used HLL scheme [7] with hydrostatic reconstruction [4]. In the case of homogeneous potential, i. e. $\nabla\phi = 0$, §5.1 and §5.2, the HLL scheme satisfies Hypothesis 1, see [7]. In the case of forcing, i.e. $\nabla\phi \neq 0$, the hydrostatic reconstruction only satisfies a semi-discrete counterpart of Hypothesis 1.ii). This is usually sufficient in practice, but to illustrate the property, a comparison with a fully entropy satisfying scheme is made, see §5.3. In §5.4, an illustration of the robustness of the strategy, on moving bottom and with dry area, it realized.

5.1 Solitary waves

It is well-known that the dispersive models (NH) and (GN) has a solitary wave solution when $\nabla\phi = 0$. More precisely, the solitary waves of (NH) and (GN) read

$$(27) \quad \begin{aligned} h(t, x) &= h^0(x) = H_0 + A \operatorname{sech}^2 \left(\sqrt{\frac{\gamma^{\text{xx}} A}{A + H_0}} \frac{x}{H_0} \right) \\ \text{and} \quad \bar{u}(t, x) &= \bar{u}^0(x) = \frac{H_0}{h(t, x)} \sqrt{g(H_0 + A)} \end{aligned}$$

with $H_0 > 0$ is the water depth far from the wave and $A > 0$ is the wave elevation. The parameter γ^{xx} depend on the model, i.e. $\gamma^{\text{NH}} = 1$ and $\gamma^{\text{GN}} = \frac{3}{4}$. The vertical velocity and the hydrodynamic pressure can be deduce using the compatibility conditions (8) and (20).

In the current section, the solution of the models with the different solitary waves is compared. More precisely we set the parameters

$$H_0 = 5 \cdot 10^{-2} \quad \text{and} \quad A = 5 \cdot 10^{-3}.$$

The computational domain is set to $[-1, 1]$. At the left boundary, the discharged is imposed and set to $h(t, -1) \bar{u}(t, -1) = h^0(-1) \bar{u}^0(-1)$ and at the right the water depth is imposed and set to $h(t, 1) = h^0(1)$.

In Figure 2, the solution of the dispersive models (NH) and (GN) initialized with the solitary wave (27) with $\gamma^{\text{xx}} = 1$ (first line) and $\gamma^{\text{xx}} = \frac{3}{4}$ (second line) is plotted at time $t = 50$ for some space steps. For small enough space step, the solitary wave of each model is well preserved by the scheme corresponding to the model. The convergence rate, about 1.5, of (GN^δ) is illustrated in Figure 3. The same result is

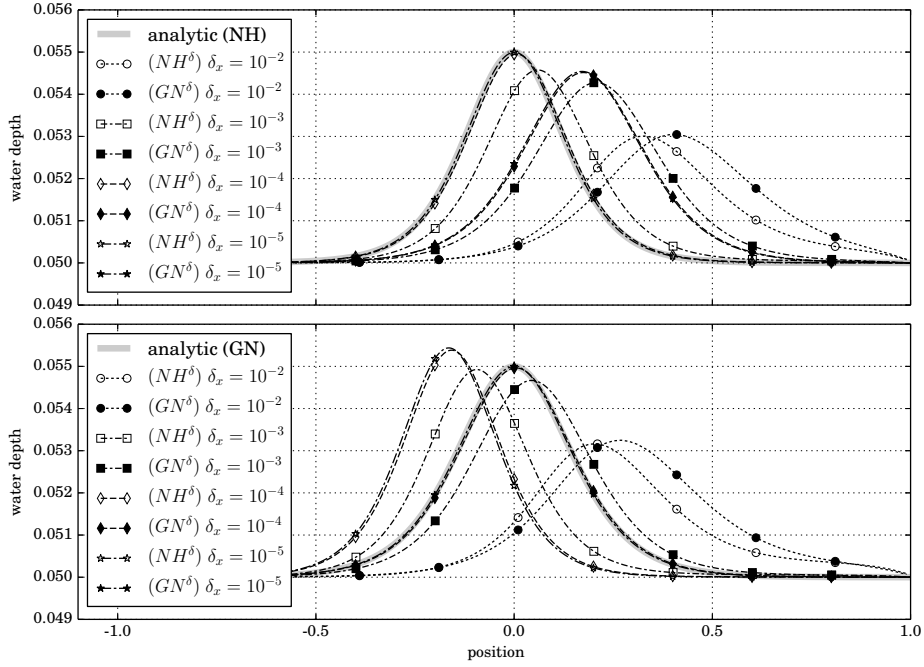


Figure 2: §5.1 Solitary waves - Water depth approximated by (NH^δ) and (GN^δ) at time $t = 50$ initialized by the solitary wave of (NH) (first line) and (GN) (second line).

observed with (NH^δ) . The supraconvergence come from the fact that the hyperbolic step (first order) is significantly less important than the dispersive step (expected second order) for this test case.

5.2 Water drop

The following test case is devoted to the parametric analysis of the aspect ratio. More precisely, (SW) is known as to be a good approximation of (E) when the aspect ratio ε is small enough. We propose to compare the dispersive model (NH) and (GN) to (SW) with respect to ε .

Let us describe the case precisely. The computational domain is set to $[0, 1]$ and the boundary conditions are walls (symmetric flow). There is no forcing $\nabla\phi = 0$ and the initial condition is set to

$$h^0(x) = \varepsilon \left(1 + e^{-100x^2}\right) \quad \text{and} \quad \bar{u}^0(x) = 0.$$

In Figure 4, the water depth approximated by each model with $\delta_x = 10^{-6}$ is plotted for several aspect ratios. The numerical diffusion probably significantly affects the solution for $\varepsilon \leq 2 \cdot 10^{-4}$. The solution of the dispersive models (NH) and (GN) are

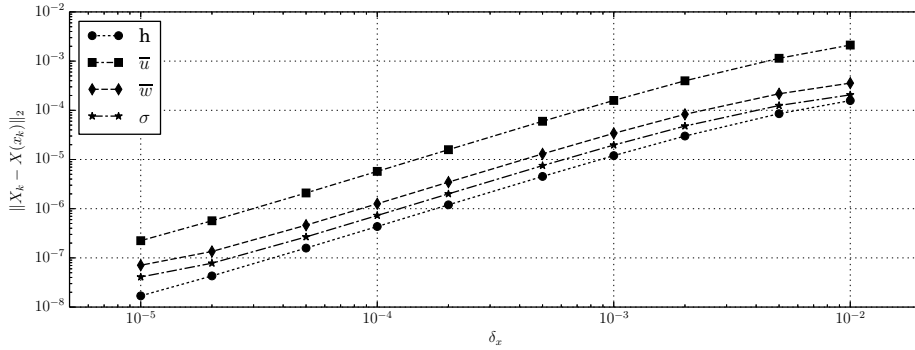


Figure 3: §5.1 Solitary waves - L^2 -norm of the difference between the numerical approximation (GN^δ) and the analytical solution (27) with $\gamma^{xx} = 3/4$ as function of the space step at time $t = 50$.

very similar, i.e. the solutions present a dispersive shock with oscillations of about twice the amplitude of the shallow water discontinuity. The frequency is slightly higher for (NH) than for (GN) even if the shape of the convex hull is the same, i.e. linear with almost the same slope. The smaller the ε , the higher the frequency of the oscillation. In Figure 5, the CPU time for each simulations is given. The slightly larger CPU time of (GN^δ) can be explained by the advection of the standard deviation.

5.3 Undular jump

A typical test case of (SW) is the transcritical stationary solution in one dimensional framework, see [11]. An analytical solution is based on the energy conservation property, i.e. Hypothesis 2.ii). More precisely, the energy conservation implies that the hydraulic head, defined by the ratio of energy flow to mass flow, i. e.

$$K^{SW} := \frac{\overline{\mathcal{G}}^h + \overline{\mathcal{G}}^{\bar{u}}}{h\bar{u}} = \phi + gh + \frac{|\bar{u}|^2}{2},$$

is piecewise constant. At the discontinuities, the jump should satisfy the Rankine-Hugoniot relation, see [11] for details. Using the same arguments, the hydraulic head of the dispersive models (NH) and (GN) respectively given by

$$K^{NH} := \frac{\overline{\mathcal{G}}^h + \overline{\mathcal{G}}^{\bar{u}} + \overline{\mathcal{G}}^{\bar{w}} + \overline{\mathcal{G}}^{q_B}}{h\bar{u}} = \phi + gh + \frac{|\bar{u}|^2}{2} + \frac{|\bar{w}|^2}{2} + \frac{q_B}{2}$$

and

$$K^{GN} := \frac{\overline{\mathcal{G}}^h + \overline{\mathcal{G}}^{\bar{u}} + \overline{\mathcal{G}}^{\bar{w}} + \overline{\mathcal{G}}^\sigma + \overline{\mathcal{G}}^{\bar{q}}}{h\bar{u}} = \phi + gh + \frac{|\bar{u}|^2}{2} + \frac{|\bar{w}|^2}{2} + \frac{|\sigma|^2}{2} + \bar{q}$$

are constant (there is no discontinuity for the dispersive models). Unfortunately, it is not possible to recover the water depth from the hydraulic head as it is for (SW). However, it is possible to compare the hydraulic head of the computed solution to the analytical value.

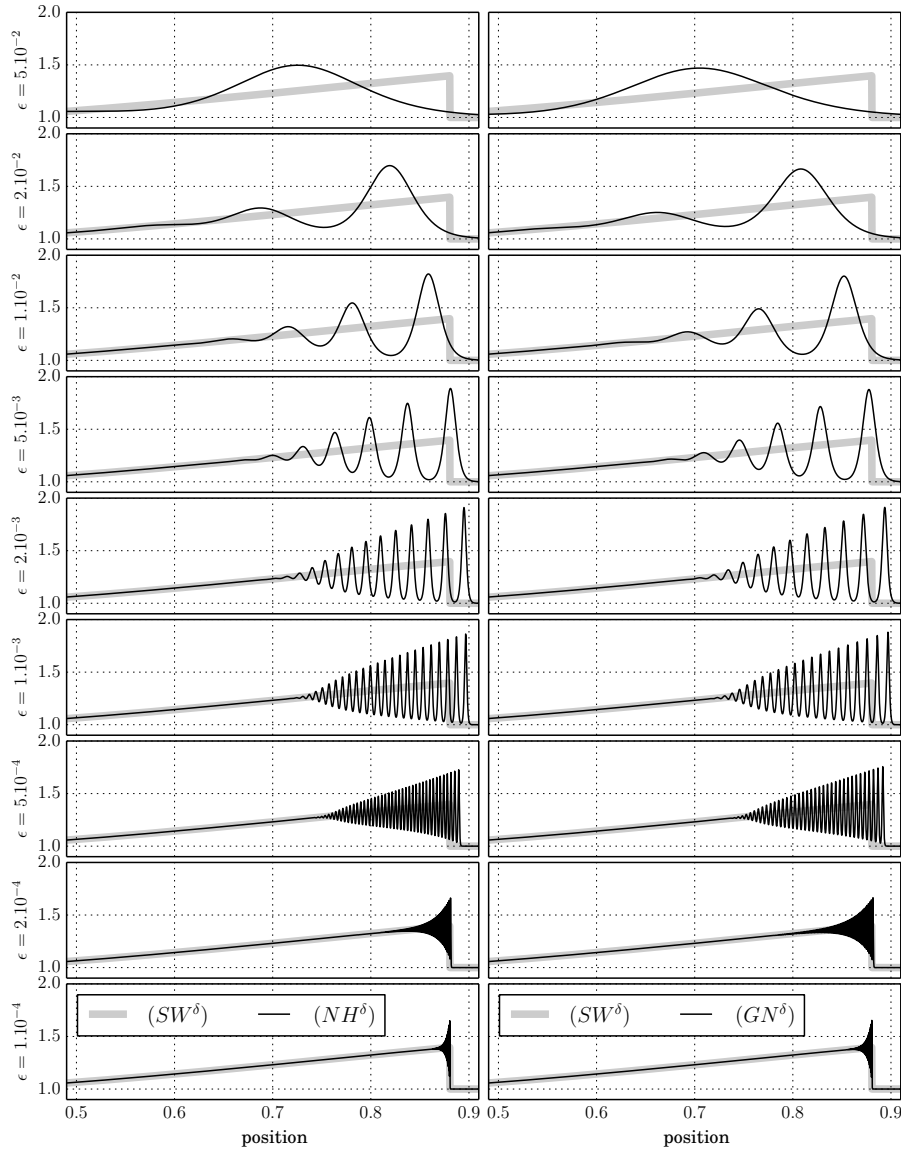


Figure 4: §5.2 Water drop - Rescaled water depth h_ϵ approximated at the rescaled time $\sqrt{g\epsilon}t = 0.6$ by (NH^δ) (left column) and (GN^δ) (right column) for several aspect ratio.

Let us describe the test case more precisely. We consider the computational domain $[0, 1]$ with an imposed discharged at the left bound $h(t, 0) \bar{u}(t, 0) = 10^{-2}$ and an imposed water depth at the right bound $h(t, 1) = 10^{-1}$. The bottom and the surface

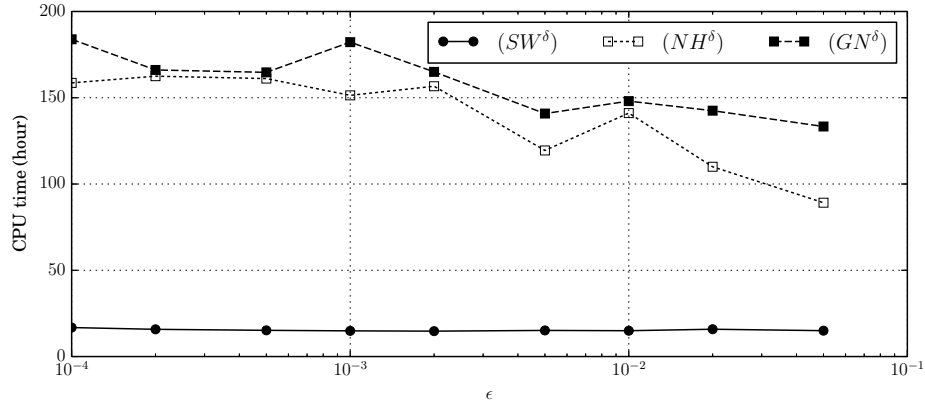


Figure 5: §5.2 Water drop - CPU time of the hierarchy of models to reach the rescaled time $\sqrt{g\epsilon}t = 0.6$ for several aspect ratio.

pressure are set to

$$B(x) = 7.5 \cdot 10^{-2} e^{-10^2(x-0.3)^2} \quad \text{and} \quad P(x) = 0.$$

Note that the converged solution is out of reach. More precisely, the better the resolution, the more oscillations extend to the right. It seems that the converged solution present periodic oscillations which does not decrease in amplitude. Thus for a fine enough resolution, the right boundary condition (fixed water depth) is no more relevant and more elaborated boundary condition are required (fixed hydraulic head).

In Figure 6, the water level and the hydraulic head computed with several schemes $YYY(XX^\delta)$ are plotted for $\delta_x = 10^{-4}$. The schemes YYY refer to the advection step. The CPR (Centered Potential Regularization) scheme [28] is entropy-satisfying, i.e. it satisfies Hypothesis 1.ii), whereas the HLL scheme with hydrostatic reconstruction satisfies only a semi-discrete counterpart of Hypothesis 1.ii). The schemes (XX^δ) refer to the dispersive step. (GN^δ) is entropy-satisfying, see Proposition 6.ii), contrary to (A.1). Only the solution $CPR(GN^\delta)$ is fully entropy-satisfying and in practice, it is the most accurate. However, the solution of $HLL(GN^\delta)$ is almost similar. In particular, the hydraulic head is still decreasing, which shows that the mechanical energy is well dissipated in this case. In the case of (A.1), the hydraulic head does not decrease and we conclude that the mechanical energy is not well dissipated. The impact on the water level is a strong numerical diffusion for both YYY schemes where the hydrodynamic effects occur.

5.4 Seawall

To illustrate the robustness of the numerical strategy for moving bottom with the dry front, the test case of the seawall is presented. The computational domain is set to $[0, 10]$ and the boundary conditions are walls. The surface pressure is neglected $P = 0$ but the bottom is a time and space function given by

$$B(t, x) = \max(0, \min(0.2(x-2), 1)) + 1.5e^{-10*(x-7)^2} + 10e^{-5(x-\min(2t,2))^2}$$

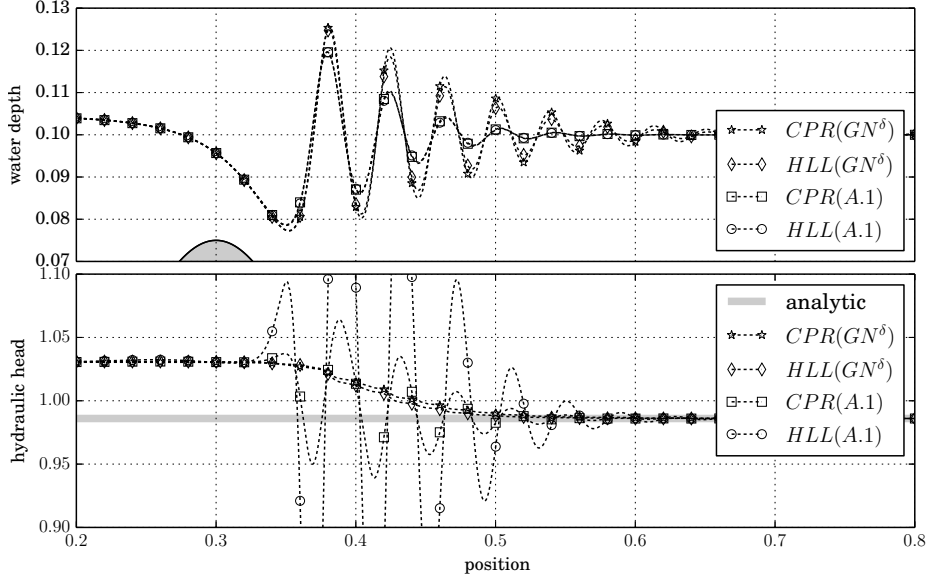


Figure 6: §5.3 Undular jump - Water level approximated (first line) and hydraulic head (second line) for several schemes.

and the initial condition reads

$$h^0(x) = \begin{cases} \max(0, 2 - B(0, x)) & \text{if } x \leq 7 \\ 0 & \text{elsewhere} \end{cases} \quad \text{and} \quad \bar{u}^0(x) = 0.$$

In Figure 7, the water level approximated with $HLL(XX^\delta)$ with $XX \in \{NH, GN\}$ and $\delta_x = 10^{-3}$ is plotted at several times. Even if the two dispersive models lead to significantly different results, especially in the dry front, they are qualitatively similar. First, we find that the dispersive models and (SW) react very differently to the bottom elevation, i.e. $0 \leq t < 1$. In the case of (SW), the water level does not become much higher than the initial condition, i.e. 3, and a wave is quickly generated. In the case of dispersive models, the water level becomes higher, i.e. it reaches 4, and the beginning of the wave is not as clear. All models pass the dike, but the shape of the free surface is different. In the case of (SW), the free surface is discontinuous before the dike and continuous after, whereas for dispersive models the free surface is continuous before the dike and discontinuous at the dry front, at least for a while. The schemes are able to deal with creation of dry or wet areas.

Conclusion

This article, the first in a series of two, focuses on numerical resolution in the multidimensional framework of a hierarchy of single-layer dispersive models. A particular attention is paid to the dissipation of mechanical energy at the discrete level, acting as a mathematical entropy. To illustrate the accuracy and the robustness of

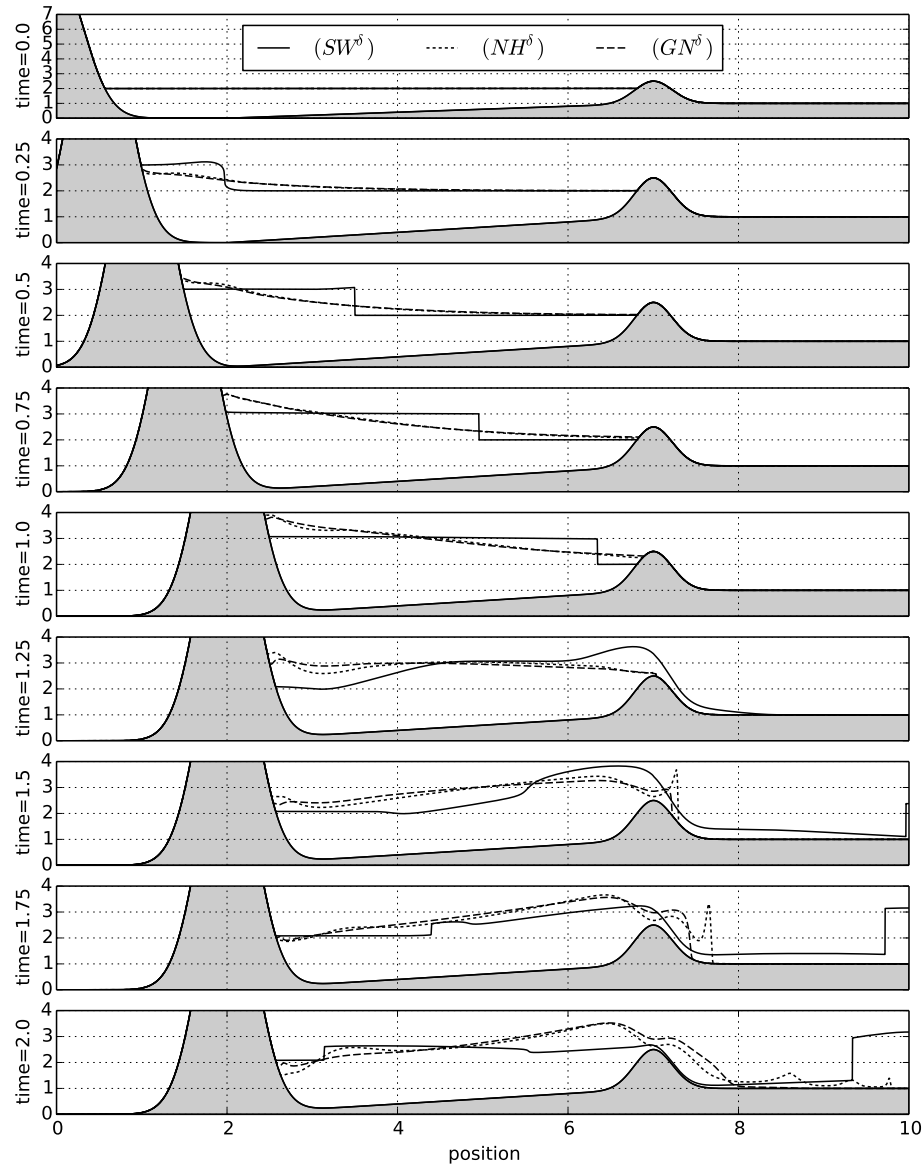


Figure 7: §5.4 Seawall - Water level approximated by the hierarchy of models at several times.

the strategy, several numerical experiments are carried out. In particular, the strategy is capable of treating dry areas.

The first perspective of this work concerns the boundary conditions. If simple boundary conditions can be prescribed as long as the hydrodynamic effects are small at the bound, some other conditions such as transparent condition or in-

coming wave are also used in practice. The second important improvement should be the analysis of the numerical equilibrium of the steady state. The lake at rest is clearly stable assuming that it is stable for (SW^δ) . However, it could be interesting to look for numerical strategy that exactly preserved at the discrete level the solitary wave §5.1. Last but not least, the numerical strategy required the resolution of a linear system that is not really analyzed in the current work. In particular, in multi-dimensional framework, a Krylov solver with well-adapted preconditioning must be proposed to allow simulations.

The second part of this work will be devoted to the layerwise dispersive models see [17]. With these schemes, we expect to illustrate the convergence of the layerwise models to solution of the free surface Euler model (E) for smooth enough solution.

Acknowledgements

I would like to thank E. D. Fernandez-Nieto, Y. Penel and J. Sainte-Marie for exchanges and discussions about the models and the different numerical strategies, the Alpines Inria project team members with in particular S. Cayrols, O. Tissot, H. Al Daas for their help with the linear algebra library (Intel® Math Kernel Library) used for this work, and E. Audusse for his kind advises. This work is a part of the research project CNRS-PICS-07480.

A Dispersion step with a compact operator

$(NH^\delta.b)$ or $(GN^\delta.b)$ are a 5-point stencil operator in one dimensional framework. One can remark that the scheme is a discretization of a reaction-advection-diffusion equation. A strategy that can be use to reduce the stencil of the scheme is to establish the reaction-advection-diffusion equation mimicking the step realized to obtain the scheme $(NH^\delta.b)$ or $(GN^\delta.b)$ at the continuous level, then use a more compact discretization. The resulting scheme reads

$$(A.1) \quad \alpha_k^{xx} \bar{u}_k^{n+1} + \nabla_k^\delta (\mu_k^{xx} \cdot \bar{u}^{n+1}) - \mu_k^{xx} \nabla_k^\delta \cdot \bar{u}^{n+1} - \frac{1}{|k|} \sum_{f \in \mathbb{F}_k} \left(\frac{\kappa_k^{xx}}{\delta_k} + \frac{\kappa_{k_f}^{xx}}{\delta_{k_f}} \right) \frac{\bar{u}_{k_f}^{n+1} - \bar{u}_k^{n+1}}{2} \cdot \mathcal{N}_k^{k_f} \mathcal{N}_k^{k_f} |f| = \beta_k^{xx}$$

with the parameters α_k^{xx} , μ_k^{xx} , κ_k^{xx} and β_k^{xx} ($xx \in \{NH, GN\}$) defined in $(NH^\delta.b)$ or $(GN^\delta.b)$ and δ_k is the compactness defined in (6). The yielding scheme (A.1) is more compact, i.e. 3-point stencil in one dimension. However, the compact scheme (A.1) does not ensure the mechanical energy dissipation and is less accurate than $(NH^\delta.b)$ or $(GN^\delta.b)$ in practice, see §5.3.

References

- [1] N. AGUILLON, E. AUDUSSE, E. GODLEWSKI, AND M. PARISOT, *Analysis of the Riemann Problem for a shallow water model with two velocities*. working paper or preprint, Oct. 2017.
- [2] N. AISSIOUENE, M.-O. BRISTEAU, E. GODLEWSKI, AND J. SAINTE-MARIE, *A robust and stable numerical scheme for a depth-averaged Euler system*. working paper or preprint, June 2015.
- [3] N. AISSIOUENE, M.-O. BRISTEAU, E. GODLEWSKI, AND J. SAINTE-MARIE, *A combined finite volume - finite element scheme for a dispersive shallow water system*, Networks and Heterogeneous Media (NHM), (2016).
- [4] E. AUDUSSE, F. BOUCHUT, M.-O. BRISTEAU, R. KLEIN, AND B. PERTHAME, *A fast and stable well-balanced scheme with hydrostatic reconstruction for shallow water flows*, SIAM J. Sci. Comput., 25 (2004), pp. 2050–2065.
- [5] E. AUDUSSE, M.-O. BRISTEAU, B. PERTHAME, AND J. SAINTE-MARIE, *A multi-layer Saint-Venant system with mass exchanges for shallow water flows. Derivation and numerical validation*, ESAIM: M2AN, 45 (2011), pp. 169–200.
- [6] P. BONNETON, F. CHAZEL, D. LANNES, F. MARCHE, AND M. TISSIER, *A splitting approach for the fully nonlinear and weakly dispersive Green–Naghdi model*, Journal of Computational Physics, 230 (2011), pp. 1479–1498.
- [7] F. BOUCHUT, *Nonlinear stability of finite volume methods for hyperbolic conservation laws, and well-balanced schemes for sources*, Springer Science & Business Media, 2004.
- [8] M.-O. BRISTEAU, A. MANGENEY, J. SAINTE-MARIE, AND N. SEGUIN, *An energy-consistent depth-averaged Euler system: Derivation and properties*, Discrete and Continuous Dynamical Systems - Series B, 20 (2015), pp. 961–988.
- [9] A. CASTRO AND D. LANNES, *Fully nonlinear long-wave models in the presence of vorticity*, Journal of Fluid Mechanics, 759 (2014), pp. 642–675.
- [10] M. CASTRO, J. M. GALLARDO, J. A. LÓPEZ-GARCÍA, AND C. PARÉS, *Well-balanced high order extensions of Godunov’s method for semilinear balance laws*, SIAM J. Numer. Anal., 46 (2008), pp. 1012–1039.
- [11] H. CHANSON, *Open-channel hydraulics*, Butterworth-Heinemann, 1959.
- [12] F. CHAZEL, D. LANNES, AND F. MARCHE, *Numerical Simulation of Strongly Nonlinear and Dispersive Waves Using a Green–Naghdi Model*, Journal of Scientific Computing, 48 (2010), pp. 105–116.
- [13] R. CIENFUEGOS, E. BARTHÉLEMY, AND P. BONNETON, *A fourth-order compact finite volume scheme for fully nonlinear and weakly dispersive Boussinesq-type equations. Part I: model development and analysis*, International Journal for Numerical Methods in Fluids, 51 (2006), pp. 1217–1253.

- [14] F. COUDERC, A. DURAN, AND J.-P. VILA, *An explicit asymptotic preserving low froude scheme for the multilayer shallow water model with density stratification*, *Journal of Computational Physics*, 343 (2017), pp. 235 – 270.
- [15] A.-J.-C. B. DE SAINT-VENANT, *Théorie du mouvement non permanent des eaux, avec application aux crues des rivières et à l'introduction des marées dans leurs lits*, *C.R. Acad. Sci. Paris*, 73 (1871), pp. 147–154.
- [16] N. FAVRIE AND S. GAVRILYUK, *A rapid numerical method for solving serre-green–naghdi equations describing long free surface gravity waves*, *Nonlinearity*, 30 (2017), p. 2718.
- [17] E. D. FERNANDEZ-NIETO, M. PARISOT, Y. PENEL, AND J. SAINTE-MARIE, *Layer-averaged approximation of Euler equations for free surface flows with a non-hydrostatic pressure*. Accepted for publication in *Commun. Math. Sci.*, hal-01324012.
- [18] J.-F. GERBEAU AND B. PERTHAME, *Derivation of viscous saint-venant system for laminar shallow water; numerical validation*, *Discrete and Continuous Dynamical Systems - Series B*, 1 (2001), pp. 89–102.
- [19] E. GODLEWSKI AND P.-A. RAVIART, *Numerical approximation of hyperbolic systems of conservation laws*, vol. 118 of *Applied Mathematical Sciences*, Springer-Verlag, New York, 1996.
- [20] S. K. GODUNOV, *A difference method for numerical calculation of discontinuous solutions of the equations of hydrodynamics*, *Mat. Sb. (N.S.)*, 47(89) (1959), pp. 271–306.
- [21] A. E. GREEN AND P. M. NAGHDI, *A derivation of equations for wave propagation in water of variable depth*, *Journal of Fluid Mechanics*, 78 (1976), pp. 237–246.
- [22] S. JIN AND X. WEN, *Two interface-type numerical methods for computing hyperbolic systems with geometrical source terms having concentrations*, *SIAM J. Sci. Comput.*, 26 (2005), pp. 2079–2101 (electronic).
- [23] D. LANNES AND P. BONNETON, *Derivation of asymptotic two-dimensional time-dependent equations for surface water wave propagation*, *Physics of Fluids*, 21 (2009).
- [24] D. LANNES AND F. MARCHE, *A new class of fully nonlinear and weakly dispersive Green–Naghdi models for efficient 2D simulations*, *Journal of Computational Physics*, 282 (2015), pp. 238–268.
- [25] O. LE MÉTAYER, S. GAVRILYUK, AND S. HANK, *A numerical scheme for the Green–Naghdi model*, *Journal of Computational Physics*, 229 (2010), pp. 2034 – 2045.
- [26] R. J. LEVEQUE, *Finite volume methods for hyperbolic problems*, vol. 31, Cambridge university press, 2002.

- [27] S. NOELLE, Y. XING, AND C.-W. SHU, *High-order well-balanced finite volume WENO schemes for shallow water equation with moving water*, J. Comput. Phys., 226 (2007), pp. 29–58.
- [28] M. PARISOT AND J.-P. VILA, *Centered-potential regularization for the advection upstream splitting method*, SIAM Journal on Numerical Analysis, 54 (2016), pp. 3083–3104.
- [29] D. H. PEREGRINE, *Long waves on a beach*, Journal of Fluid Mechanics, 27 (1967), pp. 815–827.
- [30] B. PERTHAME AND C. SIMEONI, *A kinetic scheme for the saint-venant system with a source term*, Calcolo, 38 (2001), pp. 201–231.
- [31] G. L. RICHARD AND S. L. GAVRILYUK, *A new model of roll waves: comparison with brock’s experiments*, Journal of Fluid Mechanics, 698 (2012), pp. 374–405.
- [32] ———, *The classical hydraulic jump in a model of shear shallow-water flows*, Journal of Fluid Mechanics, 725 (2013), pp. 492–521.
- [33] F. SERRE, *Contribution à l’étude des écoulements permanents et variables dans les canaux*, La Houille Blanche, (1953), pp. 830–872.
- [34] I. SULICIU, *On modelling phase transitions by means of rate-type constitutive equations. shock wave structure*, International Journal of Engineering Science, 28 (1990), pp. 829–841.
- [35] V. M. TESHUKOV, *Gas-dynamic analogy for vortex free-boundary flows*, Journal of Applied Mechanics and Technical Physics, 48 (2007), pp. 303–309.
- [36] E. F. TORO, *Riemann solvers and numerical methods for fluid dynamics: a practical introduction*, Springer Science & Business Media, 2013.
- [37] Y. YAMAZAKI, Z. KOWALIK, AND K. F. CHEUNG, *Depth-integrated, non-hydrostatic model for wave breaking and run-up*, International Journal for Numerical Methods in Fluids, 61 (2009), pp. 473–497.